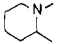
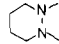

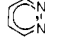


Table III. Comparison of Proton Affinities of Hydrazines and Amines

amine	PA ^a	corresponding hydrazines	PA ^a	ΔPA ^a
MeNH ₂	214.1	H ₂ NNH ₂	204.7	9.4
MeNHMe	220.6	MeHNNH ₂	214.1	6.5
Me ₂ NMe	225.1	Me ₂ NNH ₂	219.5	4.6
Me ₂ NiPr	229.8	Me ₂ NNMe ₂	224.8	5.0
	~234 ^b		229.8	ca 4
	220.8		216.2	4.6

^a kcal/mol. ^b Estimated from PA(methylpiperidine) + PA(2-methylpyridine) - PA(pyridine).

solvent exclusion. Larger alkyl groups are expected to exclude solvent from the region near the nitrogen atoms, the site of formal positive charge. Because the polarizability changes with alkyl group size increase are quite regular, one might hope to be able to separate these two factors with a large series of compounds, but will not attempt to do so with so few examples. We will defer further discussion except to point out that the low slope of the

(23) Taft, R. W.; Taagepera, M.; Abbound, J. L. M.; Wol, E. J.; DeFrees, D. J.; Hehre, W. J.; Bartmess, J. E.; McIver, R. T., Jr. *J. Am. Chem. Soc.* **1978**, *100*, 7765.

E° vs. ν IP plot is indeed principally caused by differential solvation.¹

Proton-Transfer Equilibria. A comparison of amine proton affinities with those of hydrazines which differ from the amines by replacing CH by N is given in Table III. The proton affinities are lower for the hydrazines by 9.4 kcal mol⁻¹ for H₂NNH₂, 6.5 kcal/mol for MeHNNH₂, and 4-5 kcal/mol for more highly alkylated hydrazines. There is a decrease in proton affinity expected from the electron-withdrawing effect of the second nitrogen, but we cannot separate this from other effects which may be appreciable.²⁴ We note that the decrease for pyridine vs. 1,2-diazine (last entry in Table III) is about the same as for di- and tetraalkylhydrazines, despite the difference in *n* orbital hybridization.

The far lower bond dissociation energies of protonated hydrazines than protonated amines (difference 33 ± 5 for MeNH₂ vs. H₂NNH₂, 20 ± 5 for Me₂NH vs. MeHNNH₂, 20 for Me₃N vs. Me₂NNH₂) presumably reflect the combination of inductive effects in the protonated species and resonance stabilization in the radical cations.

Registry No. H₂NNH₂, 302-01-2; MeHNNH₂, 60-34-4; Me₂NNH₂, 57-14-7; Me₂NNMe₂, 6415-12-9; *n*-PrMeNNMe₂, 60678-65-1; *n*-BuMeNNMe₂, 52598-10-4; *t*-BuMeNNMe₂, 60678-73-1; Et₂NNEt₂, 4267-00-9; hexahydro-1,2-dimethylpyridazine, 26163-37-1.

(24) (a) Bartness, J. E.; Basco, T.; Georgiadis, R. *J. Phys. Chem.* **1983**, *87*, 912. (b) Hinde, R. L.; Pross, A.; Random, L. *J. Comput. Chem.* **1980**, *1*, 118.

Chemical Derivatization of Microelectrode Arrays by Oxidation of Pyrrole and *N*-Methylpyrrole: Fabrication of Molecule-Based Electronic Devices

Gregg P. Kittlesen, Henry S. White, and Mark S. Wrighton*

Contribution from the Department of Chemistry, Massachusetts Institute of Technology, Cambridge, Massachusetts 02139. Received April 30, 1984

Abstract: An array of eight Au microelectrodes, each ~0.12 μm thick, 3 μm wide, and 140 μm long and separated from each other by a distance of 1.4 μm, has been fabricated on a 0.45 μm thick SiO₂ layer grown on a single-crystal Si substrate by use of standard microfabrication techniques. Each electrode can be individually addressed and characterized electrochemically. The individual electrodes can be functionalized with polypyrrole or with poly(*N*-methylpyrrole) by oxidation of pyrrole or *N*-methylpyrrole, respectively, using conditions similar to those for macroscopic electrodes. The amount of polymer deposited can be controlled, and it is possible to electrically "connect" adjacent microelectrodes with deposited polymer. Since the reduced forms of these polymers are insulating and the oxidized forms are electronically conducting, it is possible to prepare electronic devices that are analogous to diodes and transistors using adjacent microelectrodes connected with polymer. The current passing between two microelectrodes connected with polymer as a function of potential between them, and when both are fully oxidized to the conducting state of the polymer, allows a measure of the maximum conductivity of the polymer. We find that polypyrrole is about 10²-10³ times less resistive than poly(*N*-methylpyrrole), consistent with previous studies of these two materials. Scanning electron microscopy confirms that polymer can be grown in controlled amounts to selectively connect adjacent microelectrodes.

We wish to report the chemical functionalization of a microelectrode array in a manner that illustrates the fabrication of molecule-based electronic devices having a dimension of 1.4 μm. Our fundamental objective is to illustrate a synthetic methodology that can, in principle, lead to the preparation of aggregate chemical systems that have a specific function. Integration of chemical (and biological) systems with microelectronics seems possible inasmuch as solid-state devices now involve crucial dimensions of the same order as large molecular assemblies. A preliminary communication shows that it is possible to fabricate a molecule-based transistor using three derivatized microelectrodes.¹

This paper is a full account of the procedures used to synthesize such devices.

Our work involves the rational chemical functionalization of an array of small (nominally 2 μm wide × 140 μm long × 0.12 μm thick) Au electrodes. The nominal separation between the 2 × 140 μm Au electrodes is 2 μm. Figure 1 shows a cross-sectional view of the microelectrode array. The particular design is somewhat arbitrary, but the crucial features are that we have

(1) White, H. S.; Kittlesen, G. P.; Wrighton, M. S. *J. Am. Chem. Soc.* **1984**, *106*, 5375-5377.

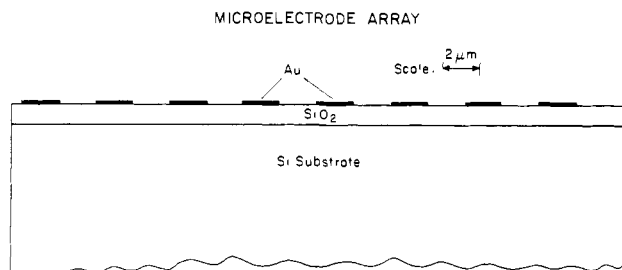


Figure 1. Cross-sectional view of design for an array of Au microelectrodes. The drawing is approximately to scale except for the Si substrate which is 0.011 in.

several small electrodes, separated by a small dimension, that can be contacted individually. The exact dimensions are not crucial except that we wish to take advantage of the small dimensions to illustrate that certain kinds of materials properties can be probed, that it is possible to independently functionalize closely spaced adjacent electrodes, and that the functionalization of such arrays can be useful in preparing new kinds of devices based on rational molecular chemistry. Some of the unique properties of microelectrodes have recently been reported in the literature.²⁻⁵ Additionally, much relevant work has been done on modification of macroscopic electrodes.⁶⁻¹⁰ We note, in particular, that work on so-called bilayer assemblies comprises part of the basis for diode devices based on redox active polymers.¹¹ One especially important piece of work is that of Pickup and Murray showing that "diodes" and "triodes" can be prepared by using macroscopic electrodes derivatized with a redox polymer and coated with a

(2) (a) Wightman, R. M. *Anal. Chem.* **1981**, *53*, 1125A-1134A. (b) Howell, J. O.; Wightman, R. M. *Anal. Chem.* **1984**, *56*, 524-529. (c) Sutts, K. J.; Dayton, M. A.; Wightman, R. M. *Anal. Chem.* **1982**, *54*, 995-998. (d) Candill, W. L.; Howell, J. O.; Wightman, R. M. *Anal. Chem.* **1982**, *54*, 2532-2535. (e) Dayton, M. A.; Brown, J. C.; Sutts, K. J.; Wightman, R. M. *Anal. Chem.* **1980**, *52*, 946-950. (f) Dayton, M. A.; Ewing, A. G.; Wightman, R. M. *Anal. Chem.* **1980**, *52*, 2392-2396.

(3) Ponchon, J.-L.; Cesuglio, R.; Gonon, F.; Jouvot, M.; Dujol, J.-F. *Anal. Chem.* **1979**, *51*, 1483-1486.

(4) Osteryoung, J.; Aoki, K. *J. Electroanal. Chem.* **1981**, *125*, 315-320.

(5) Robison, R. S.; McCreery, R. L. *Anal. Chem.* **1981**, *53*, 997-1001.

(6) (a) Murray, R. W. *Acc. Chem. Res.* **1980**, *13*, 135-141. (b) Facci, J.; Murray, R. W. *J. Electroanal. Chem.* **1981**, *124*, 339-342. (c) Daum, P.; Murray, R. W. *J. Electroanal. Chem.* **1979**, *103*, 289-294. (d) Daum, P.; Lenhard, J. R.; Rolison, D. R.; Murray, R. W. *J. Am. Chem. Soc.* **1980**, *102*, 4649-4653.

(7) (a) Peerce, P. J.; Bard, A. J. *J. Electroanal. Chem.* **1980**, *97*, 112-115. (b) Rubenstein, I.; Bard, A. J. *J. Am. Chem. Soc.* **1981**, *103*, 512-515. (c) Abruna, H. D.; Bard, A. J. *J. Am. Chem. Soc.* **1982**, *104*, 2641-2645. (d) Henning, T. P.; White, H. S.; Bard, A. J. *J. Am. Chem. Soc.* **1981**, *103*, 3937-3941. (e) Daum, P.; Murray, R. W. *J. Phys. Chem.* **1981**, *85*, 389-396.

(8) (a) Kaufman, F. G.; Schroeder, A. H.; Engler, A. H.; Kramer, S. R.; Chambers, J. B. *J. Am. Chem. Soc.* **1980**, *102*, 483-488. (b) Kaufman, F. B.; Engler, E. M. *J. Am. Chem. Soc.* **1979**, *101*, 547-549. (c) Lau, A. N. K.; Miller, L. L. *J. Am. Chem. Soc.* **1983**, *105*, 5271-5277. (d) Lau, A. N. K.; Miller, L. L.; Zinger, B. *J. Am. Chem. Soc.* **1983**, *105*, 5278-5284. (e) Van DeMark, M. R.; Miller, L. L. *J. Am. Chem. Soc.* **1978**, *100*, 3223-3224. (f) Landrum, H. L.; Salmon, R. T.; Hawkridge, F. M. *J. Am. Chem. Soc.* **1977**, *99*, 3154-3158.

(9) (a) Tsou, Y.-M.; Anson, F. C. *J. Electrochem. Soc.* **1984**, *131*, 595-601. (b) Shigehara, K.; Oyama, N.; Anson, F. C. *Inorg. Chem.* **1981**, *20*, 518-522. (c) Shigehara, K.; Oyama, N.; Anson, F. C. *J. Am. Chem. Soc.* **1981**, *103*, 2552-2558. (d) Buttry, D. A.; Anson, F. C. *J. Am. Chem. Soc.* **1983**, *105*, 685-689. (e) Oyama, N.; Anson, F. C. *J. Am. Chem. Soc.* **1979**, *101*, 3450-3456.

(10) (a) Harrison, D. J.; Daube, K.; Wrighton, M. S. *J. Electroanal. Chem.* **1984**, *163*, 93-115. (b) Dominey, R. N.; Lewis, T. J.; Wrighton, M. S. *J. Phys. Chem.* **1983**, *87*, 5345-5354. (c) Wrighton, M. S.; Palazzotto, M. C.; Bocarsly, A. B.; Bolts, J. M.; Fischer, A. B.; Nadjio, L. *J. Am. Chem. Soc.* **1978**, *100*, 7264-7271. (d) Bolts, J. M.; Wrighton, M. S. *J. Am. Chem. Soc.* **1979**, *101*, 6179-6184. (e) Bocarsly, A. B.; Walton, E. G.; Wrighton, M. S. *J. Am. Chem. Soc.* **1980**, *102*, 3390-3398. (f) Calabrese, G. S.; Buchanan, R. M.; Wrighton, M. S. *J. Am. Chem. Soc.* **1982**, *104*, 5786-5788. (g) Bookbinder, D. C.; Bruce, J. A.; Dominey, R. N.; Lewis, N. S.; Wrighton, M. S. *Proc. Natl. Acad. Sci. U.S.A.* **1980**, *77*, 6280-6284.

(11) (a) Pickup, P. G.; Kutner, W.; Leidner, C. R.; Murray, R. W. *J. Am. Chem. Soc.* **1984**, *106*, 1991-1998. (b) Abruna, H. D.; Denisevich, P.; Umana, M.; Meyer, T. J.; Murray, R. W. *J. Am. Chem. Soc.* **1981**, *103*, 1-5. (c) Denisevich, P.; Willman, K. W.; Murray, R. W. *J. Am. Chem. Soc.* **1981**, *103*, 4727-4737.

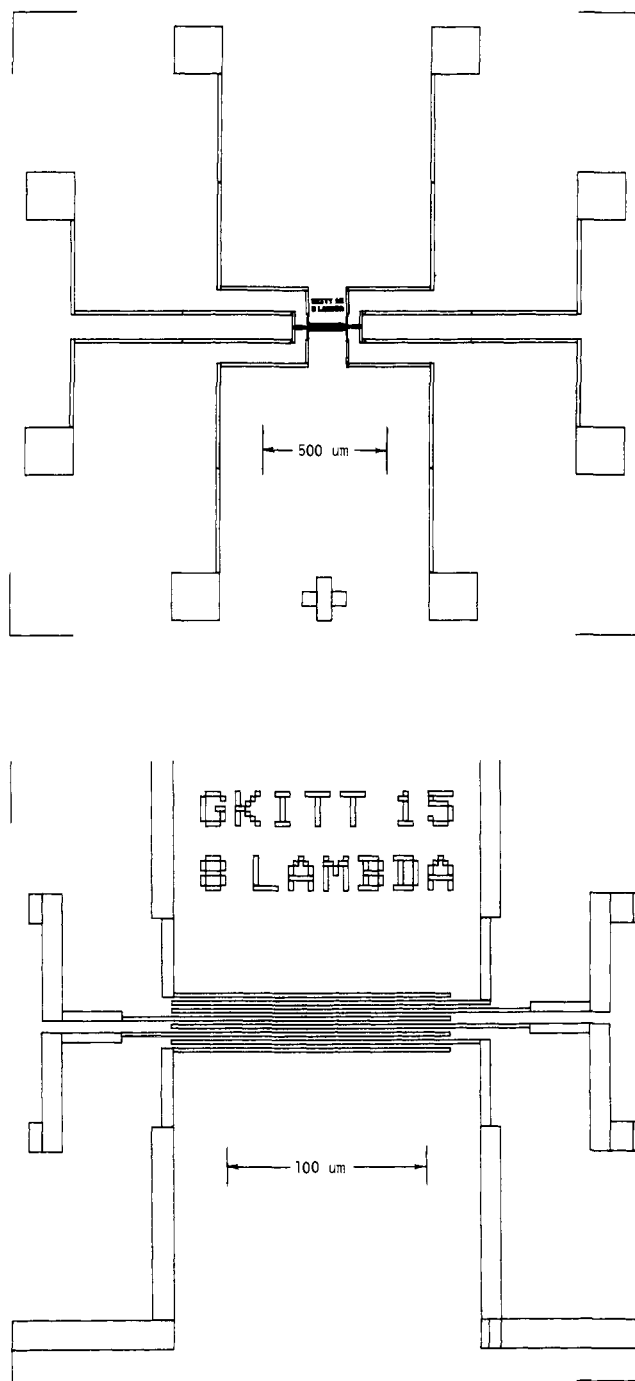


Figure 2. Top view of complete layout for microelectrode array represented in Figure 1. The drawing is to scale.

porous metal contact.¹² Also, the 2- μ m separation between the microelectrodes of the array represented in Figure 1 should allow studies of some of the polymeric materials used to modify macroscopic electrodes, since polymers of this thickness can pass significant current density in steady-state current experiments using modified electrodes.¹³

Our initial work on the microelectrode array shown in Figure 1 concerns the functionalization of the microelectrodes with conducting polymers formed from the oxidation of pyrrole and *N*-methylpyrrole at the Au surfaces. The formation of electronically conducting polypyrrole and poly(*N*-methylpyrrole) has

(12) Pickup, P. G.; Murray, R. W. *J. Electrochem. Soc.* **1984**, *131*, 833-839.

(13) (a) Lewis, T. J.; White, H. S.; Wrighton, M. S. *J. Am. Chem. Soc.*, in press. (b) Pickup, P. G.; Murray, R. W. *J. Am. Chem. Soc.* **1983**, *105*, 4510-4514.

previously been reported via oxidation of the monomers at macroscopic electrodes.¹⁴ In connection with the present work, the significant facts are that the polymers have very different conductivity in the reduced and oxidized states and that the oxidized states are sufficiently conducting that significant current can pass through a several-micrometer thickness. We seek to show that the individual microelectrodes can be functionalized in a controlled manner with a polymer and that the conductivity properties of the polymers can be exploited to make devices that have a diode characteristic with respect to current-potential behavior. Our work illustrates that it may be possible to make new kinds of electronic devices,¹⁵ including microsensor arrays,¹⁶ based on the functionalization of microelectrodes. For example, our molecule-based transistor¹ is similar to a "chemiresistor"¹⁶ that can be used to detect gases that cause a change in the resistance of a chemical coating between an interdigitated pair of electrodes.

Experimental Section

Fabrication of Microelectrode Arrays. The fabrication of microelectrode arrays was carried out in the MIT Microelectronics Laboratory equipped to prepare the completed device represented by the layout in Figure 2 with the cross-sectional view given in Figure 1. The procedure begins with the design of the array and the preparation of masks to be used in the microfabrication procedure. The microelectrode array was designed by using the computer-aided design program HPEDIT at a Hewlett-Packard Model 2648A graphics terminal on a DEC-20. The design file was translated into Caltech Intermediate Form (CIF). This CIF file was translated to Mann compatible code and written on magnetic tape. Masks for photolithography were made from the file on magnetic tape by using a Gyrex Model 1005A pattern generator. E-K 5 × 5 × 0.090 in. Extra Flat high-resolution glass emulsion plates were used to make the photolithography masks. The emulsion plates were developed by a dark-field process.

p-Si wafers of (100) orientation, 2-in. diameter, and 0.011-in. thickness obtained from Wacker were used as substrates upon which to fabricate the microelectrode arrays. The fabrication work was performed in the MIT Microelectronics Lab, a class 100 clean room. The silicon wafers were RCA cleaned in a laminar air-flow hood. The wafers were immersed in hot aqueous H₂O₂ (6% by volume)/aqueous NH₃ (14% by volume), briefly etched in HF (diluted 10:1 with deionized water), immersed in hot aqueous H₂O₂ (6% by volume)/HCl (14% by volume), rinsed in deionized water (>14 MΩ-cm), and spun dry. The cleaned wafers were loaded immediately into an oxidation tube furnace at 1100 °C under N₂. A dry/wet/dry/anneal oxidation cycle was used to grow a thermal oxide 4500 Å thick. Oxide thicknesses were measured by using a Gaertner Model L117 ellipsometer and a Nanometrics NanoSpec/AFT. The oxidized wafers were taken immediately to the photolithography stage.

Each oxidized wafer was flood-coated with hexamethyldisilazane and spun at 6000 rpm for 20 s. One milliliter of MacDermid Ultramac PR-914 positive photoresist was syringed onto each wafer. The wafer coated with resist was spun for 30 s at 4000 rpm. The wafer coated with resist was then prebaked 35 min at 90 °C.

A GCA Mann 4800 DSW Wafer Stepper was used to expose the photoresist. The Mann uses the 405-nm line of a 350-W Hg arc lamp as a light source. The mask image is reduced 5:1 in the projection printing. An exposure time of 0.85 s was used. The exposed photoresist was developed 60 s in MacDermid Ultramac MF-62 diluted 1:1 with deionized water.

A bilayer metallization was performed in a MRC 8620 Sputtering System. Wafers were placed on a quartz plate that was freshly coated with Cr. The wafers were backspattered 2 min at 50-W forward power in an Ar plasma at 5 mtorr. Cr was sputtered at 50-W forward power to give a layer 200 Å thick. Au was then sputtered at 50-W forward power to give a layer 1000 Å thick. Cr serves as an adhesion layer.

At this point Cr/Au was in contact with the SiO₂ substrate only in the areas that were to form the microelectrodes, leads, and contact pads.

The Cr/Au was deposited on photoresist in all other areas. This resist/Cr/Au on the oxide was removed by a liftoff procedure. The metallized wafers were immersed in warm acetone for 75 min. The soft-baked positive photoresist is soluble in acetone. The wafers were briefly sonicated in acetone to remove the metal between microelectrodes and dried. Wafers were then cleaned of residual photoresist in a planar oxygen plasma etching chamber at 200-W forward power in 50 mtorr of oxygen for 60 s.

Individual die (chips) were scribed and separated. The chips were mounted on TO-5 headers with Epoxi-Patch 0151 Clear (Hysol). A Mech-EI Ind. Model NU-827 Au ball ultrasonic wire bonder was used to make wire bonds from the chip to the TO-5 header. The leads, bonding pads, wire bonds, and header were encapsulated with Epoxi-Patch 0151. The header was connected through a TO-5 socket to external wires. The external wires were encased in a glass tube. The header was sealed at the distal end of the glass tube with heat-shrink tubing and Epoxi-Patch 1C white epoxy (Hysol).

Prior to use as a microelectrode array, the array was tested to establish the leakage current between the various electrodes of the array. Arrays characterized as usable have a measured resistance between any two electrodes of greater than 10⁹ Ω in nonaqueous electrolyte solution containing no added electroactive species. In many cases only a fractionation of the electrodes of an array were usable. Prior to use in experimentation the microelectrode arrays were tested further in aqueous electrolyte solution containing 0.01 M K₃[Fe(CN)₆] and 0.01 M K₄[Fe(CN)₆] to establish that the microelectrodes give the expected response. In many cases the electrodes were nonfunctioning as if covered with a layer of insulating material. Typically, a negative potential excursion to evolve H₂ cleaned the Au surface sufficiently to give good electrochemical response to the Fe(CN)₆^{3-/4-} redox couple. Under some circumstances, we have found that Cl⁻-containing media give rapid corrosion of the devices and have restricted our electrolyte to 0.1 M LiClO₄ or 0.1 M NaClO₄ in H₂O solvent or 0.1 M [*n*-Bu₄N]ClO₄ in CH₃CN solvent. Completed, tested, and cleaned arrays were used in further experiments.

Electrochemical Equipment. Most of the electrochemical experimentation was carried out by using a Pine Model RDE 3 bipotentiostat and potential programmer. In cases where two microelectrodes were under active potential control and a third was to be probed, a PAR Model 363 potentiostat/galvanostat was used in conjunction with the Pine Model RDE 3. All potentials were controlled relative to an aqueous saturated calomel reference electrode (SCE). Typically, electrochemical measurements were carried out under N₂ or Ar at 25 °C.

Derivatization of Microelectrodes. The Au microelectrodes were functionalized by oxidation of 25–50 mM pyrrole or *N*-methylpyrrole in CH₃CN/0.1 M [*n*-Bu₄N]ClO₄. The polypyrrole was deposited at +0.8 V vs. SCE, and the poly(*N*-methylpyrrole) was deposited at +1.2 V vs. SCE, as previously described.¹⁴ The deposition of the polymer can be effected in a controlled manner by removing the array from the derivatization procedure after passing a certain amount of charge. Electrodes were then examined by cyclic voltammetry in CH₃CN/0.1 M [*n*-Bu₄N]ClO₄ to assess the coverage of polymer and to determine whether the polymer coated two or more electrodes resulting in a "connection" between them.

Scanning Electron Microscopy. The microelectrode arrays were examined by electron microscopy using a Cambridge Mark 2A Stereoscan with a resolution of 20 nm. The arrays were first coated with ~200 Å of Au to minimize problems from surface charging.

Results and Discussion

Fabrication of Microelectrode Arrays. Figures 1 and 2 represent the design of the microelectrode arrays used in this study. However, the actual devices are somewhat different in certain details as illustrated by the electron micrographs shown in Figure 3. Most importantly, the Au microelectrodes are ~3 μm wide with a spacing of ~1.4 μm between them. The slightly larger electrode width is not consequential, but the smaller spacing between them allows larger currents to pass when the electrodes are "connected" with a covering of polymer (vide infra). Also, note that the outer two microelectrodes of the eight-electrode array are thinned as are some of the wires to the contact pads. The separation of the outer electrodes and the immediately adjacent electrode is still 1.4 μm, and we have found no measurable consequence from either the thinned electrode or the thinned connecting wires to the contact pads. The thinned wires are a consequence of difficulties in the metal lift-off procedure but do not affect the performance in the experiments described here. The wider Au wires yielding smaller spacings are also a consequence of the microfabrication procedure and can actually be used to

(14) (a) Kanazawa, K. K.; Diaz, A. F.; Geiss, R. H.; Gill, W. D.; Kwak, J. F.; Logan, J. A.; Rabolt, J.; Street, G. B. *J. Chem. Soc., Chem. Commun.* **1979**, 854–855. (b) Diaz, A. *Chem. Scr.* **1981**, *17*, 145–148. (c) Salmon, M.; Diaz, A. F.; Logan, A. J.; Krounki, M.; Bargon, J. *Mol. Cryst. Liq. Cryst.* **1982**, *83*, 265–276. (d) Diaz, A. F.; Martinez, A.; Kanazawa, K. K. *J. Electroanal. Chem.* **1981**, *130*, 181–187. (e) Bull, R. A.; Fan, F.-R. F.; Bard, A. J. *J. Electrochem. Soc.* **1982**, *129*, 1009–1015.

(15) See, for example, the special issue on "Molecular Electronics": *IEE J. Solid-State Electron Devices* **1983**, *103*, 197–263.

(16) For a recent overview of sensors that depend on microstructures, see: Wohltjen, H. *Anal. Chem.* **1984**, *56*, 87A–103A.

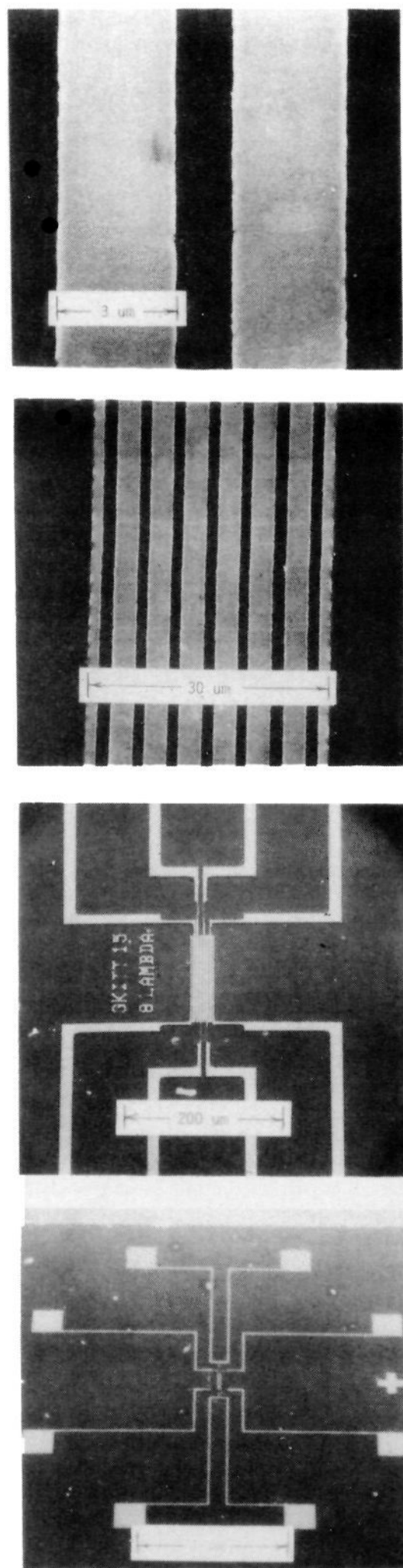


Figure 3. Scanning electron micrographs of a fabricated microelectrode array. The brighter areas in the micrographs are the Au wires and contact pads.

advantage in the study of the charge transport properties of deposited polymers.

A word about yield of useful devices is appropriate. Starting with a 2 in. diameter Si wafer yields 177 microelectrode arrays after cutting the wafer into individual chips containing the array and its contact pads. It is difficult to cite good yield data with so little in the way of statistics, but it is not uncommon to have one of every two microelectrode arrays that function properly in the test procedure that sorts out usable devices. However, it is not typical to have arrays with eight functioning electrodes for

a variety of reasons, including broken leads to contact pads, overflow of epoxy insulation, and incomplete metal liftoff. Low device yield is one of the most frustrating parts of the work described in this paper. Unlike molecular substances, there are no easy methods to "purify" chips. In principle, improvement in usable-device yield can be realized with greater attention to details in the microfabrication procedure.

In terms of the microfabrication procedure itself, the most tedious, time-consuming, and difficult task is the insulation of all exposed metal (contact pads, leads, and bonding wires) except for the eight microelectrodes. The area of desired exposure is approximately $(4 \times 10^{-3}) \times (1.5 \times 10^{-2})$ cm to allow electrolyte contact with only the eight exposed electrodes. Presently, the procedure is to use a fast-drying epoxy applied with the tip of a syringe needle by hand while observing through an optical microscope at 50 \times . This procedure works, which is its only virtue. Earlier we had attempted to define the microelectrode region with a polyimide, but we found that electrolyte could penetrate and come in contact with connecting wires and even contact pads. Future effort is to be directed toward the development of a procedure for automated, complete insulation of all metal except the microelectrode array itself.

Electrochemical Characterization of Microelectrode Arrays.

The microelectrode arrays were typically examined in H₂O/0.1 M LiClO₄/0.01 M K₃[Fe(CN)₆]/0.01 M K₄[Fe(CN)₆] to determine the electrochemical response to the Fe(CN)₆^{3-/4-} ($E^{\circ'} = +0.2$ V vs. SCE)¹⁷ redox couple. Linear potential sweep voltammograms of a good microelectrode array are shown in Figure 4. As seen in Figure 4, the linear sweep voltammogram at the 50-mV/s sweep rate shown indicates that the current is limited by diffusion of the Fe(CN)₆^{3-/4-} redox couple, and the current-potential curve characteristic of a macroscopic Au electrode for this redox couple is not seen. This is the behavior expected for electrodes having a sufficiently small dimension. Much of the work on microelectrodes and their current-potential characteristics has concerned planar disks,¹⁻⁵ but considerations of other electrode geometries suggest that the smaller dimension (3 μ m) of our rectangular electrodes is the one of consequence in assessing the sweep-rate dependence of the current-potential behavior. We will elaborate further on this issue in a separate article.

The current-potential curves in Figure 4 establish that it is possible to prepare an array of electrodes each of which can be contacted individually to give the good response to a solution species. The magnitude of the limiting current, the point-of-zero current, and the similarity of response from each of the electrodes are the points of importance. The variations in limiting current are likely a consequence of epoxy runover to varying degrees over the microelectrodes. The characterization represented by Figure 4 simply indicates that working electrodes can be fabricated and are expected to be useful in chemical derivatization studies.

Chemical Derivatization of Microelectrodes with Polypyrrole and Poly(*N*-methylpyrrole). Figure 5 represents the essential objective in functionalizing the microelectrode arrays with polymers derived from pyrrole or *N*-methylpyrrole. We seek to illustrate that it is possible to electrochemically deposit electroactive polymers on an individual electrode and in variable amounts. Most importantly, we seek to illustrate that it is possible to deposit sufficient amounts of polymer that two or more electrodes can be bridged with the polymer and thereby be "connected" to each other via the polymer. By "connected" we mean connected in the electronic sense; the consequence is that charge can pass from one microelectrode to another via conduction mechanisms of the polymer. Experiments detailed below establish that we are able to achieve the situation represented by Figure 5.

Au microelectrodes can be functionalized with polypyrrole by oxidation of 25–50 mM pyrrole in CH₃CN/0.1 M [*n*-Bu₄N]ClO₄ as described for macroscopic electrodes¹⁴ and detailed in the Experimental Section. Figure 6 shows the cyclic voltammetry

(17) Sawyer, D. T.; Roberts, J. L. "Experimental Electrochemistry for Chemistry"; Wiley: New York, 1974.

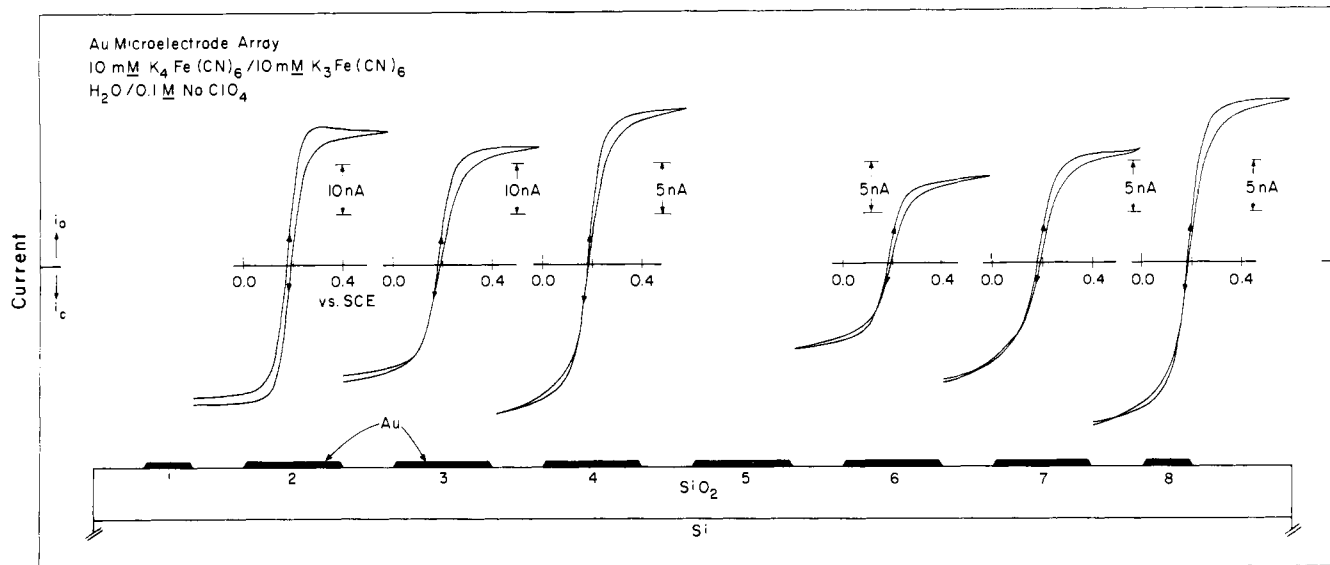


Figure 4. Linear sweep (50 mV/s) voltammograms for six of eight electrodes of a microelectrode array. Two electrodes were not connected. The entire array is immersed in $\text{H}_2\text{O}/0.1 \text{ M NaClO}_4/0.01 \text{ M K}_3[\text{Fe}(\text{CN})_6]/0.01 \text{ M K}_4[\text{Fe}(\text{CN})_6]$.

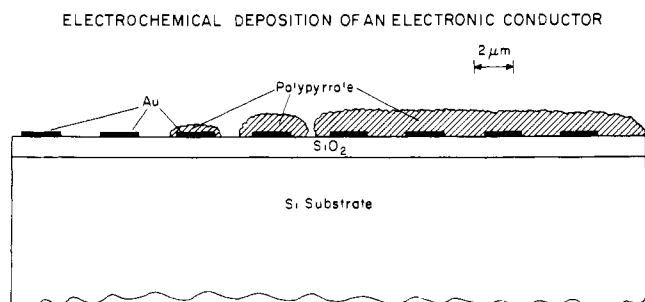


Figure 5. Representation of synthetic objective for a microelectrode array derivatized with polypyrrole. The drawing is approximately to scale.

of a polypyrrole-modified array in $\text{CH}_3\text{CN}/0.1 \text{ M } [n\text{-Bu}_4\text{N}]\text{ClO}_4$ containing no added redox-active species. Some of the eight microelectrodes were not purposefully functionalized with polypyrrole and show negligible amounts present on the basis of the lack of a cyclic voltammetry signal characteristic of electrode-confined polymer.¹⁴ Immediately adjacent to electrodes which were not derivatized are electrodes that show cyclic voltammograms characteristic of electrode-confined polypyrrole. The shape of the voltammogram is nearly the same as found for a macroscopic Au electrode derivatized in the same manner. Further, the potential of the oxidation and reduction peaks are as expected for the oxidation and reduction of polypyrrole. Controlled amounts of polypyrrole can be deposited on the basis of the integration of the charge passed upon cycling the derivatized microelectrodes individually between the negative and positive potential limits. For several of the electrodes the current-potential curves are the same and the integrated charge is large. These electrodes are covered by polypyrrole in such a way that they are connected. Typically, connected electrodes are associated with coverages of $\sim 10^{-7} \text{ mol/cm}^2$. Addressing one electrode oxidizes and reduces the polymer over all of them. This point will be elaborated fully below, but the important conclusion here is that it is possible to deposit controlled amounts of polypyrrole on a given electrode. This is an especially important point because it establishes the viability of derivatizing adjacent microelectrodes with different polymers, the subject of another article.¹⁸

In a manner similar to that for polypyrrole, it is possible to derivatize a microelectrode array with poly(*N*-methylpyrrole). Again, it is possible to derivatize in a controlled fashion and to leave some microelectrodes "naked", some with a small amount

of polymer, and some with sufficient polymer to connect two or more microelectrodes. The poly(*N*-methylpyrrole) derivatized electrodes can be characterized by cyclic voltammetry in $\text{CH}_3\text{CN}/0.1 \text{ M } [n\text{-Bu}_4\text{N}]\text{ClO}_4$ showing the oxidation and reduction of the polymer occurring at a somewhat more positive potential than for polypyrrole, as expected.¹⁴ The deposited polymers can also be observed on the microelectrodes by use of scanning electron microscopy. Figure 7 illustrates three electrodes of one array having little or no poly(*N*-methylpyrrole) on them and no obvious connection compared to three other microelectrodes on the same array having an amount of polymer sufficient to connect them. For this particular array electrochemical characterization showed that the heavily coated microelectrodes are connected and the lightly coated electrodes simply showed a cyclic voltammogram of a poly(*N*-methylpyrrole)-derivatized Au electrode. We do not, however, regard the electron microscopy as an unambiguous indicator of whether the microelectrodes are connected. We rely on the electrical and electrochemical measurements to establish this. The microscopy does reveal considerable unevenness in the coverage of the microelectrodes, perhaps as a consequence of the large ratio of length to distance of separation of the electrodes. We intend to lower this ratio to achieve greater reproducibility and evenness of coverage of the electrodes. The point here is that the long electrodes may have random, irreproducible initiation sites for polymer growth that make uneven connections between adjacent electrodes. In any event, the scanning electron microscopy is in qualitative accord with electrochemical experiments, both in terms of where polymer was supposed to have been deposited and the amounts subsequently measured by cyclic voltammetry in $\text{CH}_3\text{CN}/0.1 \text{ M } [n\text{-Bu}_4\text{N}]\text{ClO}_4$.

The electrochemical deposition procedure allows the functionalization of one microelectrode at a time, even at the 1.4- μm spacing employed in the microelectrode array. Both the microscopy and the electrochemical characterization show that there is little spreading of the polymer until sufficient quantities have been deposited that two, or more, microelectrodes are connected. Connection between two electrodes so closely spaced is what makes possible the measurement of some of the properties of the deposited polymers and the fabrication of certain kinds of electronic devices. These issues will be dealt with in the following section.

Molecule-Based Electronic Devices and Polymer Conductivity. The ability to electrically connect two, or more, microelectrodes with a polymer having very different conductivity in two redox levels raises the possibility of making new kinds of electronic devices. For the polypyrrole and the poly(*N*-methylpyrrole) the oxidized materials are electronic conductors and the reduced state is essentially insulating. The conductivity varies by a factor of more than 10^{10} , depending on the redox state of these polymers.¹⁴

(18) White, H. S.; Kittlesen, G. P.; Wrighton, M. S., manuscript in preparation.

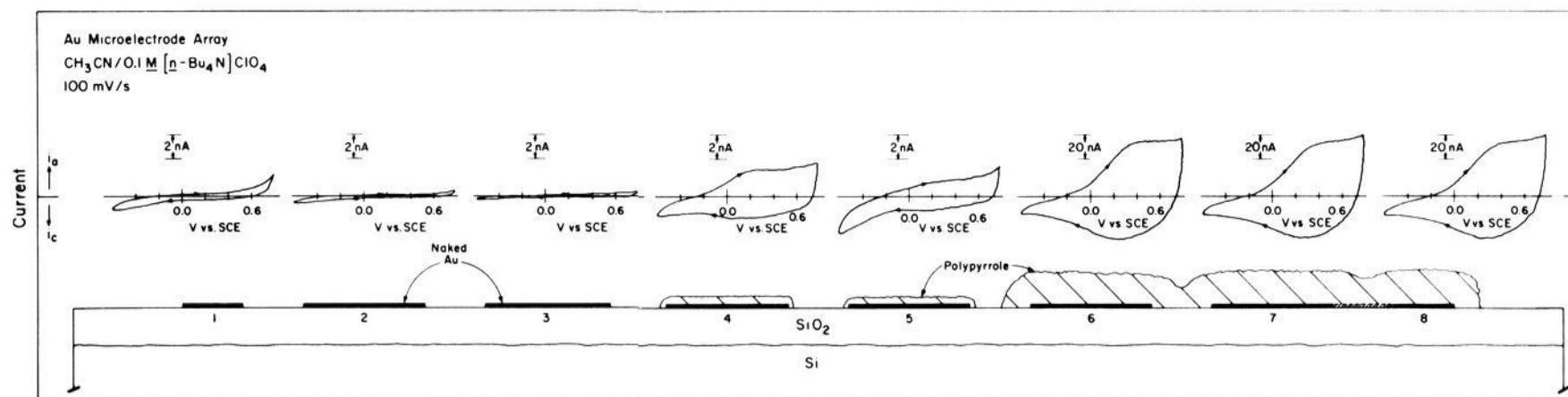


Figure 6. Cyclic voltammograms (100 mV/s) in $\text{CH}_3\text{CN}/0.1 \text{ M } [n\text{-Bu}_4\text{N}]\text{ClO}_4$ for a microelectrode array derivatized with polypyrrole. The bottom portion represents the expected situation based on the derivatization procedure and electrochemical response.

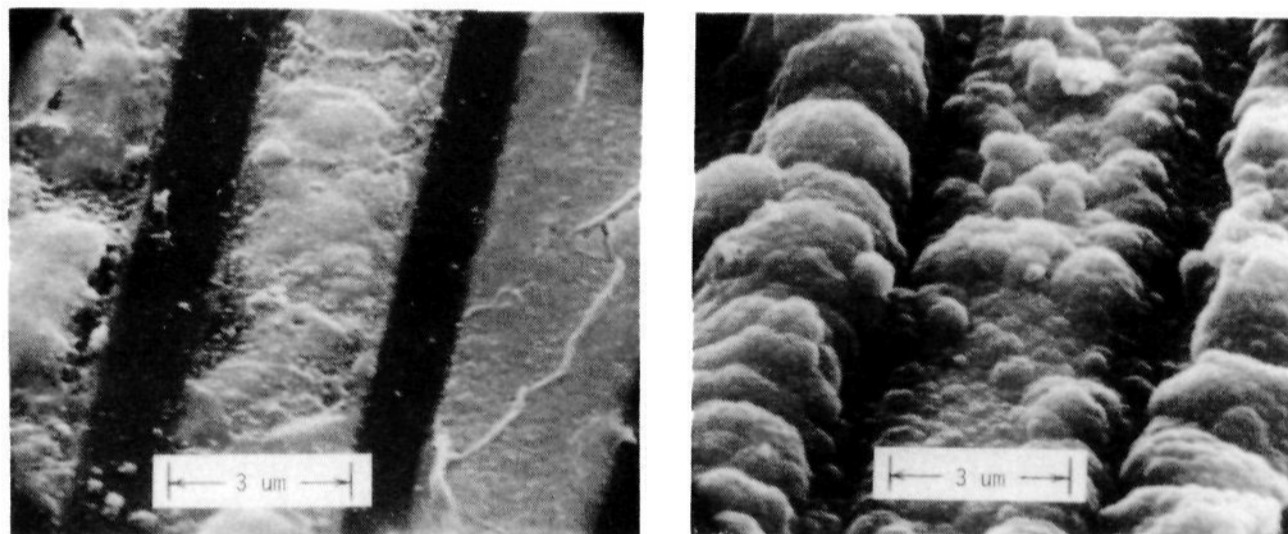


Figure 7. Scanning electron micrographs of three microelectrodes on an array lightly coated with poly(*N*-methylpyrrole) (left) and three microelectrodes on the same array heavily coated with poly(*N*-methylpyrrole) (right). Electrochemical measurements show that the left three electrodes are unconnected and the right three are connected.

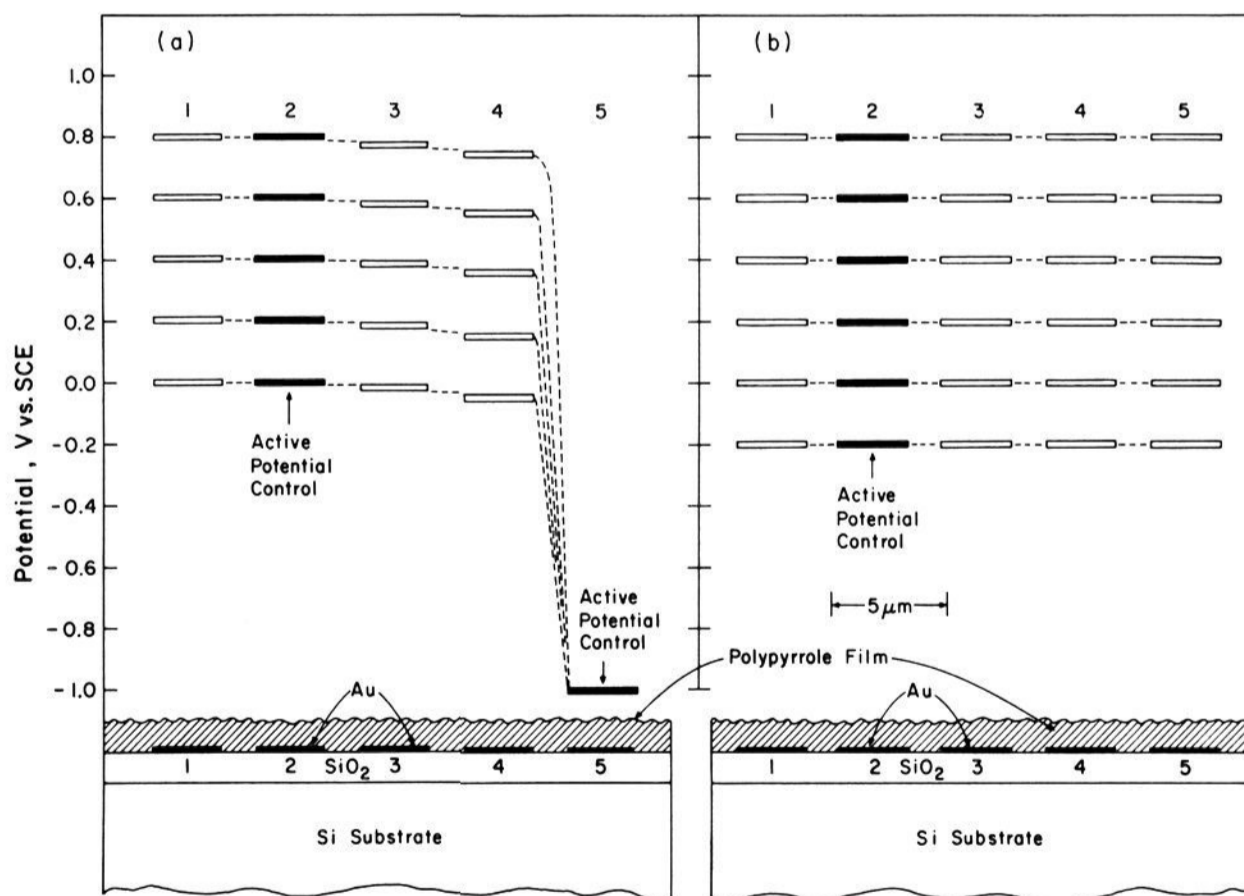


Figure 8. (a) Potential of five electrodes connected with polypyrrole when one is under active potential control at -1.0 V vs. SCE and one is at a positive potential where the polypyrrole is expected to be conducting. (b) Potential of same five electrodes in (a) but only one electrode is under active potential control. In both (a) and (b) the microelectrode array is immersed in $\text{CH}_3\text{CN}/0.1 \text{ M } [n\text{-Bu}_4\text{N}]\text{ClO}_4$.

We have undertaken experiments that show that these conductivity properties can be measured using heavily coated microelectrode arrays and that the current passing between two connected microelectrodes as a function of the potential between them can vary as for a diode. The threshold potential of the diode and the current-potential curve depend on the polymer.

Figure 8 summarizes the results of an experiment using a microelectrode array where five electrodes are connected using

polypyrrole. The experiment is to determine the spatial potential distribution across the polypyrrole-coated microelectrode array when one or two of the electrodes is under active potential control. The entire array is immersed in $\text{CH}_3\text{CN}/0.1 \text{ M } [n\text{-Bu}_4\text{N}]\text{ClO}_4$, and a bipotentiostat is used to actively control the potential of one or two microelectrodes against a common reference electrode and counterelectrode in the solution. To establish that the microelectrodes are connected we set the potential of one (electrode 5

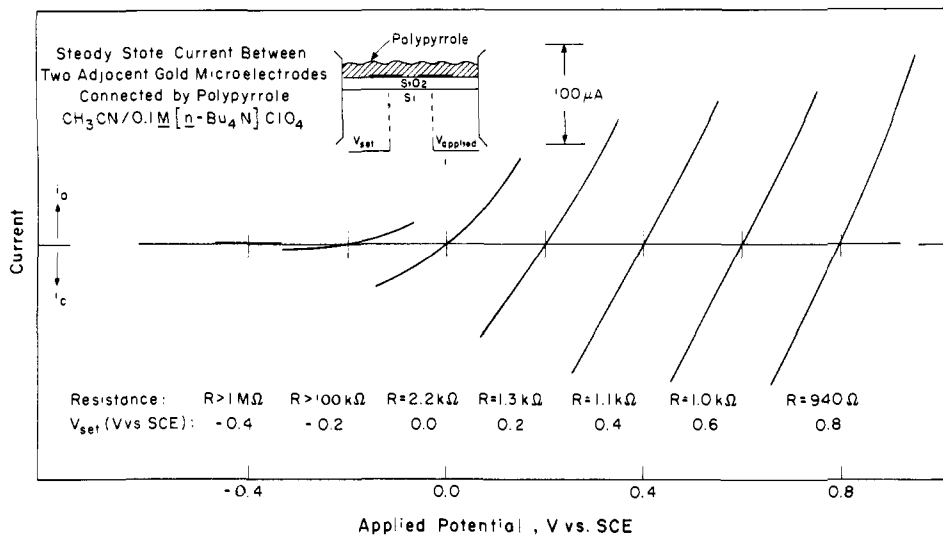


Figure 9. Current vs. V_{appl} curves for two adjacent microelectrodes connected with polypyrrole as a function of V_{set} where V_{set} is the potential of one of the two electrodes fixed vs. SCE. The potential, V_{appl} , of the other electrode is varied. The current measured is that between the two microelectrodes.

in Figure 8a) of the five electrodes at a negative potential, -1.0 V vs. SCE, and one (electrode 2 in Figure 8a) at a variable positive potential and measure the potential of the microelectrodes not under active potential control. As shown in Figure 8a all of the electrodes, except for the one under active control at -1.0 V vs. SCE, are nearly equal to the positive potential applied to electrode 2. A small potential drop (~ 50 mV) occurs over the $\sim 9\text{-}\mu\text{m}$ distance separating electrodes 2 and 4, but the essential finding is that nearly all (up to 1.8 V) of the potential drop occurs across a narrow region immediately adjacent to electrode 5 under active potential control at -1.0 V. This result is consistent with the difference in conductivity¹⁴ of the reduced and oxidized states of polypyrrole. The consequence of the extreme difference in conductivity with redox state is that the potential drop can occur across a very small fraction of length of the connecting polymer when one microelectrode is held at a potential where the polymer is reduced and insulating and another is held at a potential where the polymer is oxidized and conducting. Such would not be expected for a polymer having only modest conductivity, as for polymers that exhibit so-called redox conductivity, where a linear change in concentration of redox centers across the thickness spanned by two electrodes at differing potentials would give a potential profile predicted by the Nernst equation.^{13b,19} The experiment represented by Figure 8 illustrates part of the value of the microelectrode array in that a polymer film can be probed at small spatial intervals. Figure 8b shows that when only one of the microelectrodes is under active potential control in the positive region all of the electrodes are measured to be at the same potential as would be expected when there is an electrical connection between them. When one of the microelectrodes is driven negative it would be expected that all would ultimately follow, but upon reduction the polymer becomes insulating and the rate of potential following can be expected to be slower.

Figure 9 shows current-potential data which establish that diode behavior from polypyrrole-connected microelectrodes does obtain. What is shown is a family of current vs. V_{appl} curves as a function of the potential, V_{set} , at which one of the electrodes is fixed relative to the SCE. The current measured is that passing between the two microelectrodes. We have established that the magnitude of the current passing through one microelectrode is identical with that passing through the other microelectrode but opposite in sign. Note that when V_{set} is sufficiently positive that the current- V_{appl} curve is linear over a wide range of V_{appl} ; the resistance of polypyrrole from the slope of such plots is about $10^3 \Omega$. When V_{set} is sufficiently negative, there is a broad range of the current- V_{appl} curve where there is insignificant current. Thus, for a value of

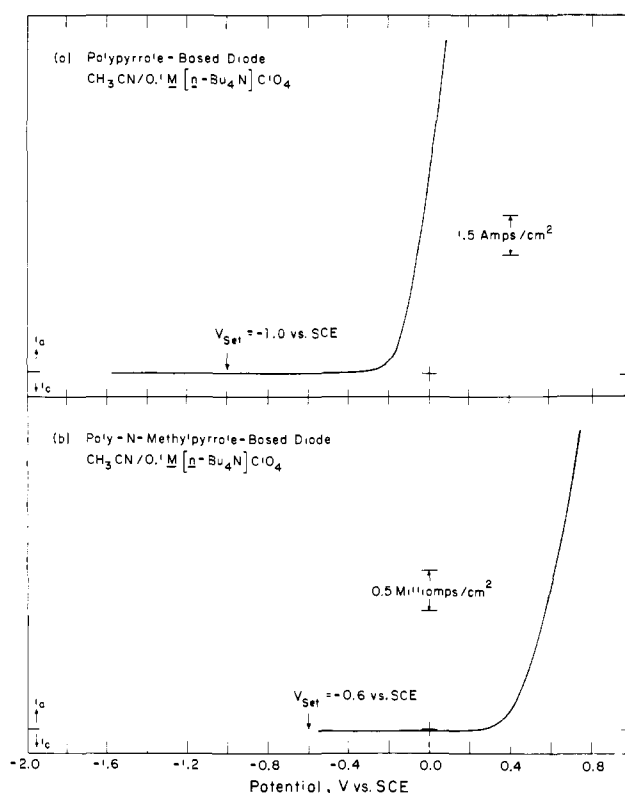


Figure 10. Comparison of diode characteristic for two microelectrodes connected with (a) polypyrrole and (b) poly(*N*-methylpyrrole). In (a) $V_{\text{set}} = -1.0$ V vs. SCE and in (b) $V_{\text{set}} = -0.6$ V vs. SCE.

V_{set} sufficiently negative, a good diode characteristic can be obtained (Figure 10). The onset of current corresponds closely to the situation where the V_{appl} results in the conversion of the polypyrrole from its reduced and insulating state to its oxidized and strongly conducting state, as would be expected.

It is interesting that we are able to observe steady-state current densities exceeding 1 kA/cm^2 for two Au microelectrodes connected by polypyrrole. This current density is calculated by using the exposed geometrical area of a Au electrode. The unevenness of the polymer in terms of the coverage and degree of connection between two adjacent Au electrodes makes it difficult to establish the current density in the film. However, the 1 kA/cm^2 is a lower limit, since the thickness of the polymer is $\sim 1 \mu\text{m}$.

Data similar to those shown in Figure 9 for polypyrrole have also been obtained for two microelectrodes connected with poly-

(19) Andrieux, C. P.; Saveant, J. M. *J. Electroanal. Chem.* **1982**, *142*, 1-30.

(*N*-methylpyrrole). However, the value of V_{set} necessary to obtain a current that is linear with variation in V_{appl} is more positive than with polypyrrole and the resistance of the poly(*N*-methylpyrrole) is 10^5 – $10^6 \Omega$. Both the higher resistance and the more positive potential necessary to obtain the conducting regime are consistent with the known differences between the two polymers.¹⁴ Two adjacent microelectrodes connected with poly(*N*-methylpyrrole) can function as a diode also (Figure 10). We see that the threshold potential is greater than for the polypyrrole, consistent with the more positive potential needed to bring the poly(*N*-methylpyrrole) to its maximum conductivity state. The current densities for the diodes represented by the data in Figure 10 are high, and especially so for the polypyrrole device. This is a consequence of the close spacing of the electrodes, coupled with the reasonable conductivity of the polymers. The diode characteristics illustrated in Figure 10 show an impressive direct current–potential relationship. It should be noted, though, that the on–off rate will be determined by chemical reactions of the polymer. The on–off rate for the polypyrrole and poly(*N*-methylpyrrole) devices described here is ~ 10 s. The curves in Figures 9 and 10 are essentially steady state (< 5 mV/s). Fast sweep rates give fast turnon but slow turnoff, resulting in large hysteresis in the current–potential curves.

For both the polypyrrole and the poly(*N*-methylpyrrole) we have estimated the actual conductivities of the oxidized polymers from several measurements on independently prepared microelectrode arrays having two or more electrodes connected with the polymer. The values are $\sim 10^{-2}$ and $\sim 10^{-4}$ – $10^{-5} \Omega^{-1}\text{cm}^{-1}$ for the polypyrrole and the poly(*N*-methylpyrrole), respectively, in fair agreement with the range of conductivities reported in the literature.¹⁴ The relative conductivity of the polypyrrole and poly(*N*-methylpyrrole) is also in accord with what is known about these two polymers. Greater confidence is placed in the relative conductivity of the two polymers, rather than in absolute values, because the dimensions and geometry are not accurately known.

The “diode” devices described here are different from a solid-state diode,²⁰ e.g., a p–n junction or a semiconductor/metal Schottky barrier. The solid-state devices, in addition to having capability of high-frequency operation, are two-terminal devices. In effect, the molecule-based diodes characterized here are, in fact, triodes where the ability to pass current in only one direction (as for a diode) depends on fixing one of the terminals to a potential, V_{set} , relative to the SCE. Thus, the solution represents a third terminal. This relationship has been pointed out by Pickup and Murray¹² for a macroscopic diode/triode based on a redox polymer. Work is under way in this laboratory to fabricate a two-terminal molecule-based diode by derivatizing adjacent microelectrodes with two different redox polymers such that the two polymers do connect. Dissimilar values of $E^{\circ'}$ for the two connected polymers will allow current to flow in only one direction without the restriction of having active potential control of one of the terminals, as for the devices described here.

In some respects, the diode/triode devices described here resemble solid-state transistors²⁰ where V_{set} is the analogue of the gate potential, V_G , and V_{appl} is the drain potential, V_D . A difference, of course, is that in the solid-state devices the potentials are referenced to ground whereas the potentials for the devices described here are referenced to a reference electrode immersed in the solution. The charge passed associated with movement in V_{set} from a negative potential where the polymer is insulating to a positive potential where the polymer is conducting can be regarded as the signal (charge) necessary to turn the device “on”.

The data in Figure 9 for a polypyrrole-based device shows that the device starts to turn on between a V_G of -0.4 and -0.2 V vs. SCE. This is the analogue of the threshold voltage, V_T , for a solid-state device and corresponds to the potential where polypyrrole becomes conducting. Solid-state transistors do not, however, have a diode-like V_D vs. drain current, I_D , characteristic. Thus, the molecule-based devices do differ in important ways compared to solid-state devices.

In a recent communication¹ we referred to an array of three microelectrodes connected with polypyrrole as a molecule-based transistor. In that device one of the three electrodes was regarded as the gate with the other two being source and drain, but the values of V_D and V_G were not referenced to a common point as in the diode/triode described here or a solid-state transistor. The value of V_G was referenced to an SCE. A floating potential was used at the source and drain; V_D was set with a battery. The value of V_T , however, was also between -0.4 and -0.2 V vs. SCE, since fundamentally all of the devices described based on polypyrrole or poly(*N*-methylpyrrole) depend on the dramatic change in conductivity in going from the reduced to the oxidized state of the polymer. The rationale for characterizing the derivatized three-electrode array with a floating V_D is to simulate the response of the device to a redox reagent in solution that could be equilibrated with the polymer to turn it “on” or “off”. Future effort in this laboratory will include study of the equilibration of molecule-based transistors with solution redox reagents.

Conclusions

We have shown that it is possible to fabricate a microelectrode array and to functionalize the individual microelectrodes in a controlled fashion using an electropolymerization procedure. Diodes having a crucial dimension (contact to contact) of $1.4 \mu\text{m}$ have been demonstrated for two different polymers, polypyrrole and poly(*N*-methylpyrrole). The diode characteristics depend in a rational way on the polymer used to connect two microelectrodes. This work and our report of a molecule-based transistor establish that synthetic strategies do exist for the integration of chemical and microelectronics systems.¹ The synthetic strategy of electropolymerization has been shown to have widespread utility,^{6a,7a,c,10b,g,11a,13a,21} and we expect that many of the polymers deposited on macroscopic electrodes can be deposited onto electrodes spaced as closely as $1.4 \mu\text{m}$. In principle, the microelectrode arrays functionalized with the conducting polymers employed here could serve as redox sensors, since the conductivity depends on the redox state of the polymer. However, we have not yet made any quantitative measurements in this regard.

Acknowledgment. We thank the Defense Advanced Research Projects Agency and the Office of Naval Research for partial support of this research. Support from the MIT Polymer Processing Program and use of the MIT Microelectronics Laboratory in the Center for Materials Science and Engineering are gratefully acknowledged.

Registry No. SiO₂, 7631-86-9; Si, 7440-21-3; Au, 7440-57-5; [*n*-Bu₄N]ClO₄, 1923-70-2; K₃Fe(CN)₆, 13746-66-2; K₄Fe(CN)₆, 13943-58-3; NaClO₄, 7601-89-0; pyrrole, 109-97-7; *N*-methylpyrrole, 96-54-8; polypyrrole (homopolymer), 30604-81-0; poly(*N*-methylpyrrole) (homopolymer), 72945-66-5.

(20) Sze, S. M. “Physics of Semiconductor Devices”, 2nd ed.; Wiley: New York, 1981.

(21) (a) Trouillon, G.; Garnier, F. *J. Electroanal. Chem.* **1982**, *135*, 173–178. (b) Noufi, R.; Nozik, A. J.; White, J.; Warren, J. *J. Electrochem. Soc.* **1982**, *129*, 2261–2265. (c) Simon, R. A.; Ricco, A. J.; Wrighton, M. S. *J. Am. Chem. Soc.* **1982**, *104*, 2031–2034. (d) Bookbinder, D. C.; Wrighton, M. S. *J. Electrochem. Soc.* **1983**, *130*, 1080–1087.